

MAGELLANIC-CLOUD-TYPE INTERSTELLAR DUST ALONG LOW DENSITY SIGHTLINES IN THE GALAXY

GEOFFREY C. CLAYTON¹, KARL D. GORDON², AND MICHAEL J. WOLFF³

accepted ApJS, Aug 2000, in press

ABSTRACT

We have studied the UV extinction properties along 30 Galactic sightlines using data from the *International Ultraviolet Explorer* (IUE) archive that have never been previously examined. These distant ($d > 1$ kpc) sightlines were selected to investigate the distribution and physical conditions of gas located in low density regions of the Galactic disk and halo. The average densities along these sightlines are extremely low. It is likely that they are dominated by the warm intercloud medium and have little contribution from the cold cloud medium. We find that a subsample of these sightlines has extinction curves with weak bumps and very steep far-UV extinction reminiscent of the Magellanic clouds. These sightlines all lie in the region bounded by $325^\circ \leq l \leq 0^\circ$ and $-5^\circ \geq b \geq -11^\circ$. The gas along these sightlines shows forbidden velocities which may indicate that the dust has been subject to shocks. This type of low density sightline may mimic the environments found in the Magellanic Clouds. Large values of $N(\text{Ca II})/N(\text{Na I})$ indicating low depletion are associated with steep far-UV extinction. A possible correlation exists between decreasing bump strength and increasing far-UV steepness for extinction curves in the Galaxy and the Magellanic Clouds.

1. INTRODUCTION

There is an average Milky Way extinction relation, $A(\lambda)/A(V)$, over the wavelength range $0.125 \mu\text{m}$ to $3.5 \mu\text{m}$, which is applicable to a wide range of interstellar dust environments, including lines of sight through diffuse dust, and dark cloud dust, as well as dust associated with star formation (Cardelli, Clayton, & Mathis 1989 (CCM); Cardelli & Clayton 1991; Mathis & Cardelli 1992; Fitzpatrick 1999). The existence of this relation, valid over a large wavelength interval, suggests that the environmental processes which modify the grains are efficient and affect all grains. The CCM relation depends on only one parameter, the ratio of total-to-selective extinction, R_V which is a crude measure of the size distribution of interstellar dust grains.

However, the CCM relation does not appear to apply beyond the Milky Way. It does not always fit the observed extinction along sightlines observed in the Magellanic Clouds and M31 (e.g., Clayton & Martin 1985; Fitzpatrick 1985, 1986; Clayton et al. 1996; Bianchi et al. 1996; Gordon & Clayton 1998; Misselt, Clayton, & Gordon 1999). The 2175 \AA bump is weaker and the far-UV extinction is steeper in many of the Magellanic cloud sightlines but there are also sightlines in both the LMC and SMC where the dust extinction does follow CCM. The few lines of sight studied in M31 seem to show a CCM-like far-UV extinction and a weak 2175 \AA bump (Bianchi et al. 1996). On the other hand, the starburst nucleus of M33 appears to be associated with Milky-Way-type dust (Gordon et al. 1999). The variations in extinction properties seen in the Magellanic Clouds and M31 may be due to several

factors. Different environments, such as star formation regions where large amounts of UV radiation and shocks are present, may play a large role in processing dust. Evidence for this can be seen in the LMC where two distinct wavelength dependences of UV extinction have been found for dust inside and outside the supergiant shell, LMC 2, which lies on the southeast side of 30 Dor. This structure was formed by the combined stellar winds and supernovae explosions from the stellar association at its center (Misselt et al. 1999). In the SMC, the dust properties are even more extreme, showing extinction curves for three of four sightlines which have virtually no bump and are very steep in the far-UV (Gordon & Clayton 1998). Although the dust responsible for these curves is located near regions of star formation in the SMC, the environment is likely to be less severe than for the LMC 2 dust. The 30 Dor region, where LMC 2 is located, is a much larger star forming region than any in the SMC. The dust environments in starburst galaxies and QSOs, which also show SMC-like extinction, are much more extreme than 30 Dor (e.g., Gordon, Calzetti, & Witt 1997; Pitman, Clayton & Gordon 2000; Gordon, Smith & Clayton 2000). The SMC has star formation occurring at only 1% the rate of a starburst galaxy so other factors such as the known differences in metallicity between galaxies may be important (Fitzpatrick 1986; Gordon & Clayton 1998; Misselt et al. 1999).

Setting aside global metallicity differences, are there sightlines in the Galaxy where the dust environment is similar to those seen in the Magellanic clouds? Real deviations from CCM are seen in the Galaxy but deviations

¹Department of Physics & Astronomy, Louisiana State University
 Baton Rouge, LA 70803
 Email: gclayton@fenway.phys.lsu.edu

²Steward Observatory, University of Arizona, Tucson, AZ 85721
 Email: kgordon@as.arizona.edu

³Space Science Institute, 1540 30th Street, Suite 23 Boulder, CO 80303-1012
 Email: wolff@colorado.edu

of the kind seen in the Magellanic clouds have been seen only rarely (Cardelli & Clayton 1991; Mathis & Cardelli 1992). A few sightlines (e.g., 62542, 204827, and 210121) show weak bumps and anomalously strong far-UV extinction for their measured values of R_V . Their extinction curves are plotted in Figure 1. These deviant sightlines represent a variety of dust environments. The Galactic sightline toward HD 62542 is somewhat similar to LMC 2. Its dust was swept up by bubbles blown by two nearby O stars (Cardelli & Savage 1988). HD 204827 is also in a star formation region where the dust has been subject to shocks (Clayton & Fitzpatrick 1987). HD 210121 lies behind a single cloud in the halo. There is no present activity near this cloud although it was ejected into the halo at some time in the past. There are some important differences between these Galactic extinction curves and those in the Magellanic clouds. The bump seen for HD 62542 is not just weak but it is very broad and shifted to the blue (Cardelli & Savage 1988). Mantles on the bump grains has been suggested as the reason for the weak, broad, and shifted Galactic bumps (Mathis & Cardelli 1992; Mathis 1994). These sightlines show that dust in a variety of environments with a range of R_V values can have extinction curves similar to those in the LMC. However, none of the anomalous Galactic sightlines, seen in Figure 1, approach the SMC extinction properties. The SMC dust has weaker bumps and steeper far-UV extinction than any known Galactic or LMC sightline.

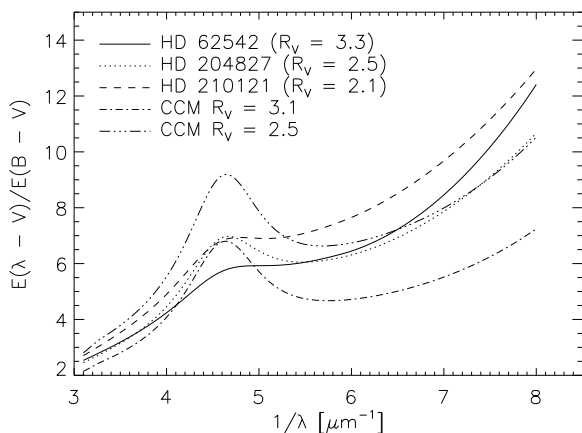


FIG. 1.— Sightlines in the Galaxy showing anomalous extinction. CCM curves for R_V values of 2.5 and 3.1 are plotted for comparison.

Most of the Galactic sightlines, that have been studied previously, differ in one respect from the LMC and SMC sightlines. They are significantly more reddened than the Magellanic cloud sightlines. In particular, those sightlines showing the greatest deviations from CCM, those near the supershell LMC 2 and those in the SMC, all have $E(B-V) < 0.25$. Of the twenty-nine CCM sightlines only two have $E(B-V) < 0.30$. The others range up to $E(B-V) = 1.2$. Similarly, the Fitzpatrick & Massa sample of eighty stars includes only seven with $E(B-V) < 0.30$ (Fitzpatrick & Massa 1990; Fitzpatrick 1999). Therefore, the dust along the Magellanic cloud sightlines is more diffuse and more representative of the warm intercloud medium than the cold cloud medium which is better represented in the Galactic samples.

Kiszkurno-Koziej & Lequeux (1987) suggest from ANS extinction measurements of 1200 stars in the Galaxy that there may be a correlation between UV extinction parameters and distance from the Galactic plane. As $|z|$ increases, the bump becomes weaker and the far-UV extinction stronger. These sightlines have low reddenings and long sightlines so they are also more diffuse and therefore more like those in the Magellanic clouds. To investigate whether the extinction properties observed in the Magellanic clouds are related to the diffuse nature of the sightlines, a sample of long sightlines with low reddenings in the Galaxy was chosen and UV data were obtained with the *International Ultraviolet Explorer* (IUE) so that extinction curves could be constructed.

2. THE SAMPLE

Sembach, Danks, & Savage (1993) obtained high resolution Na I D and Ca II K spectra for a sample of distant ($d > 1$ kpc) stars. These sightlines were selected to investigate the distribution and physical conditions of gas located in low density regions of the Galactic disk and halo. The sightlines listed in Table 1 were selected from the Sembach et al. sample for a complementary study of the UV extinction properties of interstellar dust in low density conditions. The Sembach et al. sample is limited to stars with spectral types between O8 and B3 which makes them ideal for extinction studies. Following the definitions of Sembach et al. the sightlines in Table 1 lie outside the Sagittarius spiral arm (IA1), between the Sagittarius and Scutum-Crux spiral arms (IA2), beyond the Scutum-Crux arm toward the Galactic center (GC), and the inner 4 kpc of the Galaxy (IGC). The stars lie at distances ranging from 1.5 to 9.5 kpc and have heights above or below the plane of 0 to 1.5 kpc. Twelve of the sightlines extend into the Galactic halo, defined as $|z| > 500$ pc. The locations of these stars in the Galaxy are plotted in Figure 1 of Sembach et al. (1993).

3. EXTINCTION CURVES

Low dispersion short and long wavelength IUE spectra were obtained between 1991 and 1994 by Jason Cardelli. The spectra listed in Table 2 were downloaded from the IUE archive. The archive spectra were reduced using NEWSIPS and then were recalibrated using the method developed by Massa & Fitzpatrick (2000). The short and long wavelength spectra for each star were co-added, binned to the instrumental resolution (~ 5 Å) and merged at the maximum wavelength of the short wavelength spectrum.

Extinction curves were constructed using the standard pair method (e.g., Massa, Savage & Fitzpatrick 1983). Uncertainties in the extinction curves contain terms that depend both on the broadband photometric uncertainties as well as those in the IUE fluxes, which are calculated directly in NEWSIPS. Our error analysis is described in detail in Gordon & Clayton (1998). The sample includes early type supergiants which may be used with the same accuracy as main sequence stars in calculating extinction (Cardelli, Sembach, & Mathis 1992). We required $\Delta(B - V) \geq 0.14$ between the reddened and comparison stars to minimize the uncertainties. The comparison stars have been dereddened as described by Cardelli et al.

TABLE 1
LOW DENSITY INTERSTELLAR SIGHTLINES IN THE GALAXY

<i>HD</i>	<i>SpT</i>	<i>V</i>	<i>E_{B-V}</i>	<i>l</i>	<i>b</i>	<i>d</i>	<i>z</i>	<i>Type</i>	<i>n_o(HI)</i>	<i>N(CaII)/N(NaI)</i>
HD 64219	B2.5 III	9.72	0.17	241.99	0.94	3.46	0.06	IA1	0.098	0.49
HD 69106	B0.5 IV _{nn}	7.13	0.18	254.52	-1.33	1.49	-0.03	IA1	0.235	0.21
HD 93827	B1 Ibn	9.31	0.23	288.55	-1.54	8.31	-0.22	IA2	0.064	0.45
HD 94493	B1 Ib	7.23	0.20	289.01	-1.18	3.33	-0.07	IA1	0.121	0.66
HD 97848	O8 V	8.68	0.30	290.74	1.53	2.69	0.09	IA2	0.225	0.50
HD 100276	B0.5 Ib	7.16	0.26	293.31	0.77	2.96	0.04	IA2	0.172	0.38
HD 103779	B0.5 Iab	7.20	0.21	296.85	-1.02	4.02	-0.07	IA2	0.104	0.54
HD 104683	B1 Ib	7.92	0.19	297.74	-1.97	4.64	-0.16	IA2	0.090	0.79
HD 104705	B0 Ib	7.76	0.26	297.45	-0.34	3.90	-0.02	IA2	0.128	0.67
HD 113012	B0.2 Ib	8.12	0.34	304.21	2.77	4.11	0.20	IA2	0.188	0.50
HD 148422	B1 Ia	8.60	0.28	329.92	-5.60	8.84	-0.86	GC	0.125	0.72
HD 151805	B1 Ib	8.91	0.32	343.20	1.59	5.94	0.16	IGC	0.119	0.34
HD 151990	O9 IV	9.46	0.39	334.99	-5.54	4.47	-0.43	GC	0.244	0.69
HD 158243	B1 Iab:	8.15	0.19	337.59	-10.64	6.49	-1.20	IGC	0.145	0.63
HD 160993	B1 Iab:	7.73	0.21	345.61	-8.56	5.20	-0.77	IGC	0.149	0.63
HD 161653	B1 II	7.11	0.26	352.42	-5.26	1.82	-0.17	IA2	0.315	...
HD 163522	B1 Ia	8.46	0.19	349.57	-9.09	9.42	-1.49	IGC	0.119	1.11
HD 164019	O9.5 III	9.26	0.53	1.91	-2.62	3.83	-0.28	GC	0.308	...
HD 164340	B0.2 III	9.25	0.15	352.06	-8.60	5.46	-0.82	IGC	0.105	0.95
HD 165582	B1 II	9.33	0.24	357.49	-6.96	5.21	-0.63	IGC	0.152	0.85
HD 167402	B0 Ib	8.95	0.23	2.26	-6.39	7.04	-0.78	IGC	0.121	0.79
HD 168941	O9.5 II-III	9.34	0.37	5.82	-6.31	5.79	-0.64	IGC	0.212	<0.38
HD 172140	B0.5 III	9.96	0.22	5.28	-10.61	6.85	-1.26	IGC	0.165	0.82
HD 177989	B0 III	9.33	0.25	17.81	-11.88	4.91	-1.01	GC	0.223	<0.25
HD 178487	B0 Ia	8.66	0.40	25.78	-8.56	7.66	-1.14	IGC	0.249	<0.31
HD 179407	B0.5 Ib	9.41	0.31	24.02	-10.40	7.76	-1.40	IGC	0.224	<0.39

TABLE 2
OBSERVATIONS

Star	Standard	SpT	$\Delta(B-V)$	SWP spectra	LWR/LWP spectra
HD 64219	HD 31726	B1V	0.20	SWP 47546	LWP 25410/25412
HD 69106	HD 63922	B0III	0.21	SWP 11114/47547	LWR 8825
HD 93827	HD 62747	B1.5III	0.29	SWP 48392/48400	LWP 26160
HD 94493	HD 119159	B0.5III	0.29	SWP 47548/47571	LWP 25413/25420
HD 97848	HD 47839	O7V	0.29	SWP 39231	LWP 18380
HD 100276	HD 64760	B0.5Ib	0.25	SWP 39256	LWP 18397
HD 103779	HD 64760	B0.5Ib	0.22	SWP 48391/48399	LWP 26159/26170
HD 104683	HD 119159	B0.5III	0.28	SWP 47560	LWP 25414/25424
HD 104705	HD 63922	B0III	0.28	SWP 39257	LWP 18398
HD 113012	HD 63922	B0III	0.41	SWP 47559	LWP 25423
HD 148422	HD 64760	B0.5Ib	0.30	SWP 48329	LWP 26100
HD 151805	HD 40111	B1Ib	0.34	SWP 39267	LWP 18408
HD 151990	HD 188209	O9.5Ia	0.34	SWP 47555/47570	LWP 25419
HD 158243	HD 91316	B1Iab	0.19	SWP 48328	LWP 26099
HD 160993	HD 40111	B1Ib	0.21	SWP 48334	LWP 26105/26109
HD 161653	HD 62747	B1.5III	0.25	SWP 47542	LWP 25406
HD 163522	HD 91316	B1Iab	0.19	SWP 48335	LWP 26106
HD 164019	HD 167756	B0Ia	0.45	SWP 33407/47543	LWP 13140/13141/25416/25417
HD 164340	HD 119159	B0.5III	0.14	SWP 47541/47552	LWP 25441
HD 165582	HD 119159	B0.5III	0.28	SWP 48336	LWP 26107
HD 167402	HD 167756	B0Ia	0.20	SWP 42336	LWP 21095
HD 168941	HD 63922	B0III	0.34	SWP 33409/47540	LWP 13142/25404
HD 172140	HD 119159	B0.5III	0.24	SWP 48341	LWP 26110/26172
HD 177989	HD 119159	B0.5III	0.23	SWP 42342	LWP 21110
HD 178487	HD 167756	B0Ia	0.38	SWP 48413/48415	LWP 26186
HD 179407	HD 150168	B1Ia	0.28	SWP 42334	LWP 21093/21096

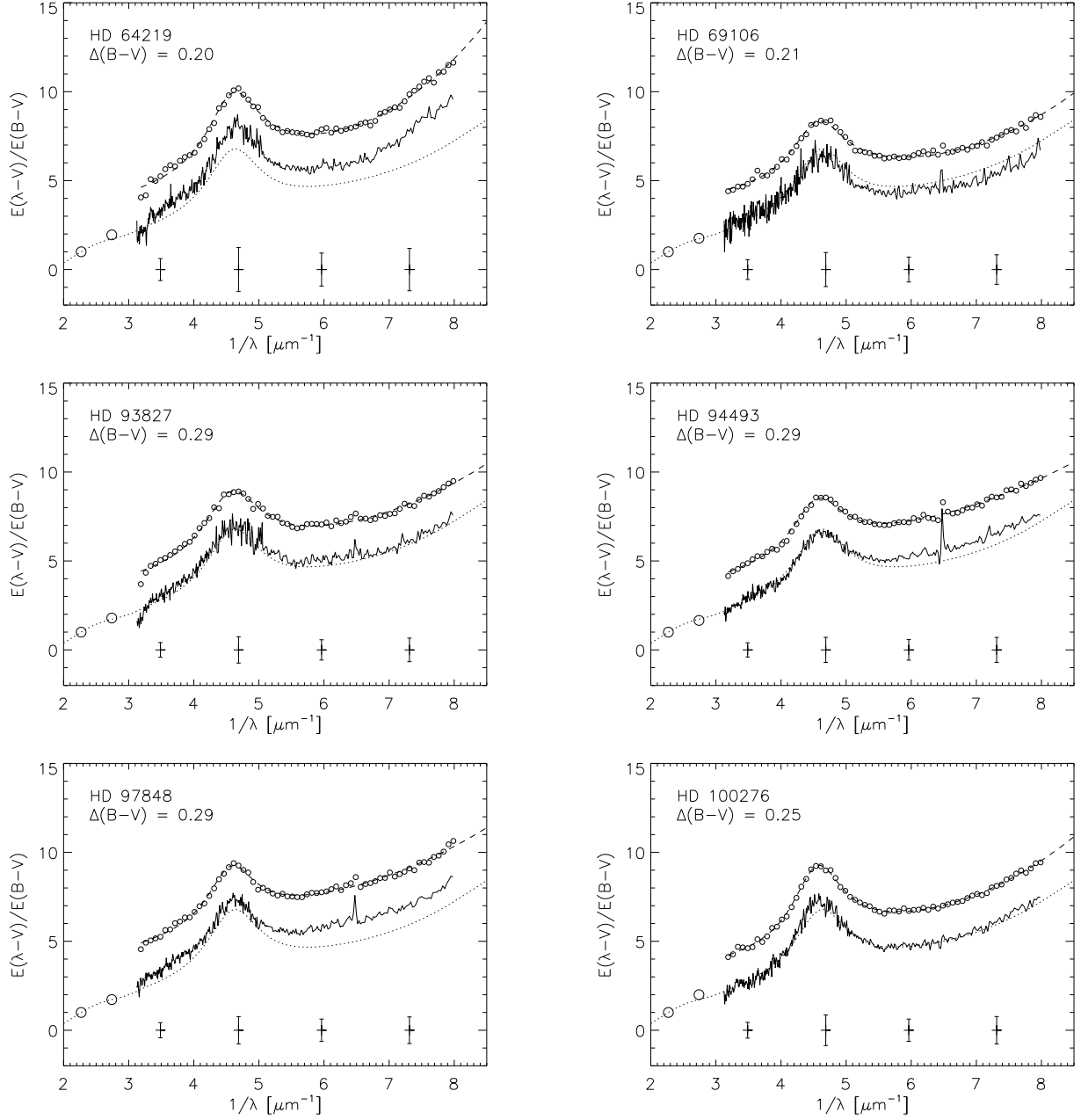


FIG. 2.— Extinction curves for the stars in the sample. Each panel shows the calculated extinction curve (solid line), smoothed curve (small open circles, offset two units for clarity), FM fit (dashed line), CCM relation for $R_V=3.1$ (dotted line), and extinction in the U and B bands (large open circles). One sigma error bars for the unsmoothed extinction curve are plotted at four representative wavelengths. The value of $\Delta(B-V)$ between the reddened and comparison stars is listed.

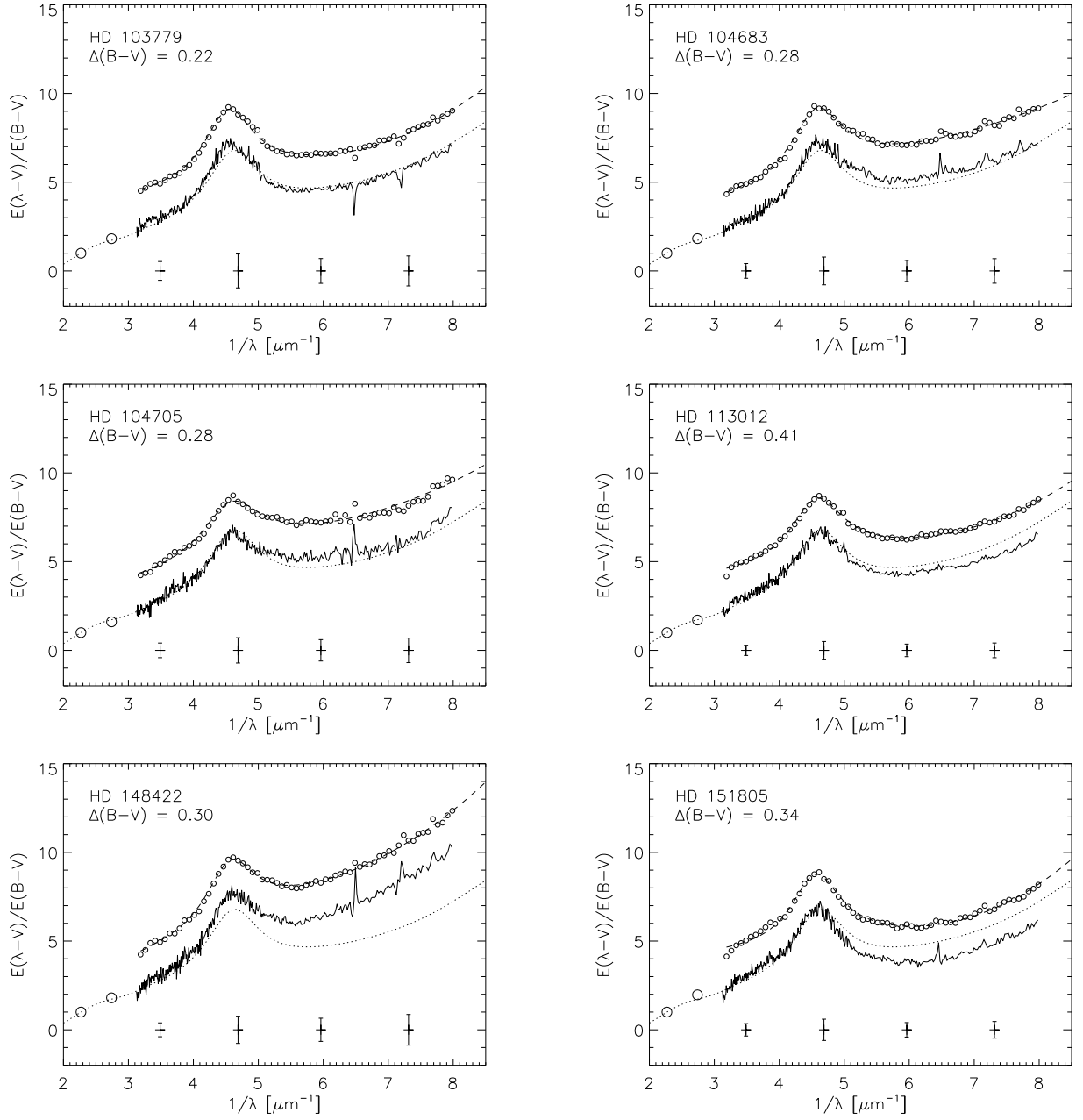


FIG. 2 (CONT.).— Extinction curves for the stars in the sample.

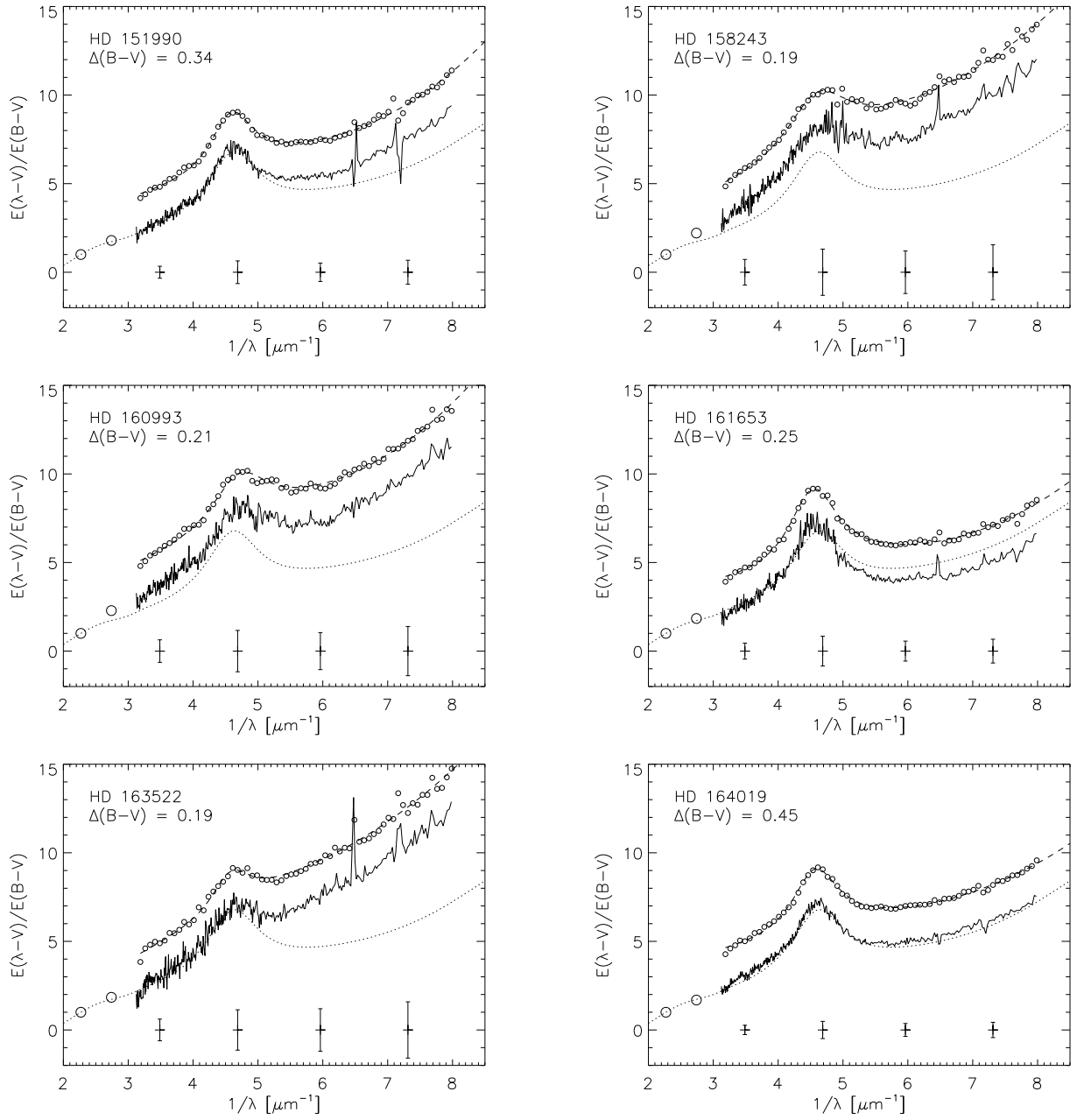


FIG. 2 (CONT.).— Extinction curves for the stars in the sample.

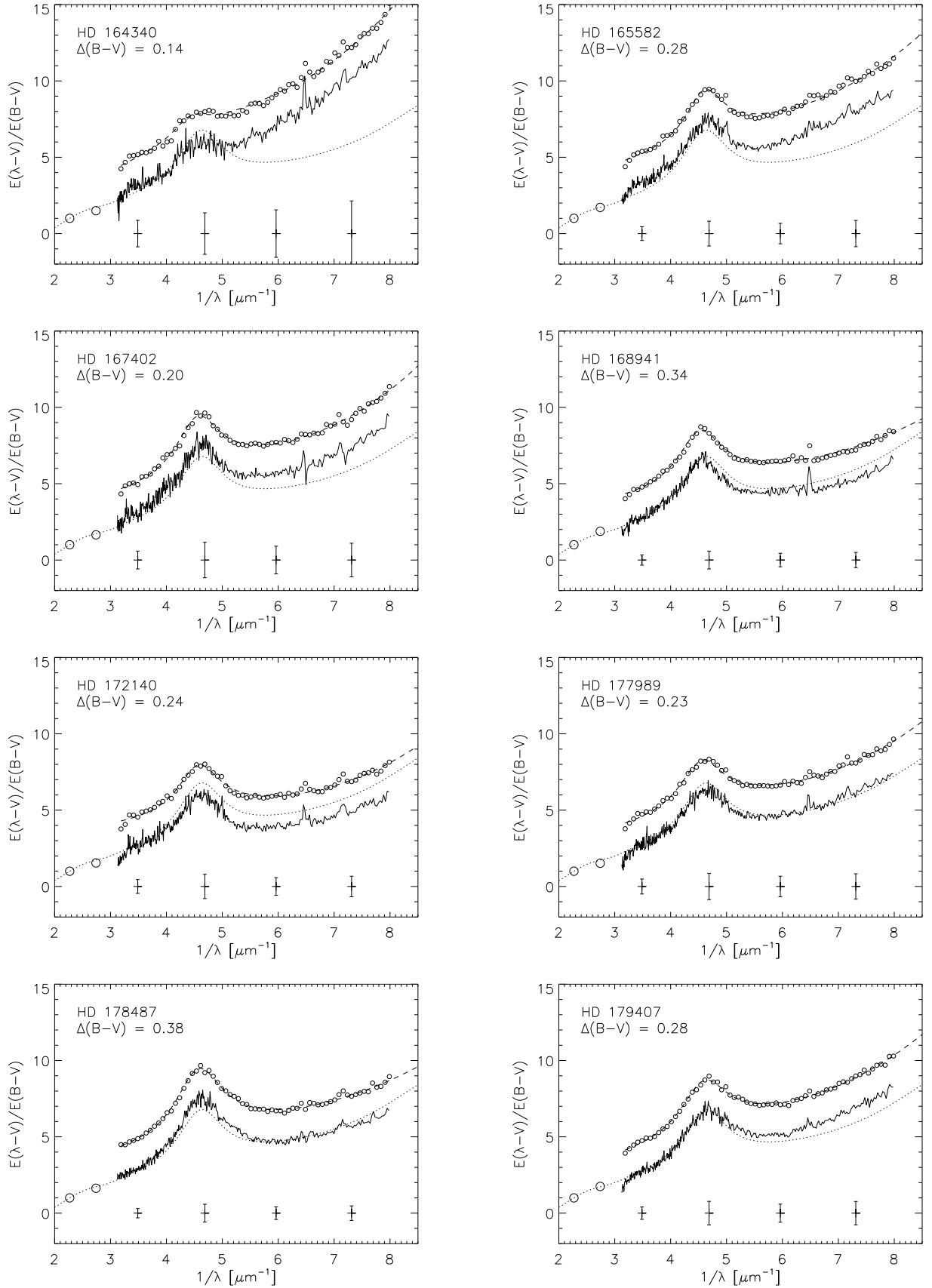


FIG. 2 (CONT.).— Extinction curves for the stars in the sample.

TABLE 3
FM PARAMETERS

Star	c_1	c_2	c_3	c_4	x_o	γ
Low Density Sample						
HD 64219	-0.83 ± 0.22	0.98 ± 0.10	4.36 ± 0.33	0.93 ± 0.14	4.61 ± 0.01	1.01 ± 0.03
HD 69106	0.40 ± 0.29	0.58 ± 0.06	3.40 ± 0.26	0.55 ± 0.06	4.58 ± 0.01	1.01 ± 0.03
HD 93827	-0.54 ± 0.15	0.83 ± 0.07	4.18 ± 0.14	0.40 ± 0.03	4.59 ± 0.01	1.07 ± 0.03
HD 94493	-0.95 ± 0.08	0.97 ± 0.08	2.75 ± 0.17	0.26 ± 0.02	4.57 ± 0.01	0.95 ± 0.01
HD 97848	-0.32 ± 0.17	0.95 ± 0.07	2.57 ± 0.15	0.34 ± 0.04	4.58 ± 0.01	0.89 ± 0.01
HD 100276	-0.66 ± 0.18	0.81 ± 0.07	3.69 ± 0.20	0.55 ± 0.07	4.57 ± 0.01	0.93 ± 0.02
HD 103779	0.31 ± 0.18	0.63 ± 0.08	3.46 ± 0.37	0.57 ± 0.04	4.54 ± 0.02	0.93 ± 0.00
HD 104683	-0.75 ± 0.12	0.91 ± 0.08	3.62 ± 0.14	0.19 ± 0.02	4.59 ± 0.01	0.98 ± 0.02
HD 104705	-0.86 ± 0.14	0.92 ± 0.07	3.89 ± 0.15	0.30 ± 0.03	4.59 ± 0.01	1.13 ± 0.03
HD 113012	0.64 ± 0.18	0.54 ± 0.03	3.51 ± 0.11	0.49 ± 0.03	4.59 ± 0.01	1.00 ± 0.02
HD 151805	1.26 ± 0.15	0.35 ± 0.04	3.48 ± 0.27	0.71 ± 0.03	4.57 ± 0.01	0.94 ± 0.01
HD 161653	0.05 ± 0.27	0.57 ± 0.04	3.93 ± 0.19	0.55 ± 0.06	4.55 ± 0.01	0.93 ± 0.02
HD 164019	-0.00 ± 0.13	0.76 ± 0.04	2.84 ± 0.08	0.43 ± 0.03	4.58 ± 0.01	0.88 ± 0.01
HD 167402	-0.78 ± 0.20	1.00 ± 0.11	3.28 ± 0.20	0.63 ± 0.10	4.56 ± 0.01	0.94 ± 0.03
HD 168941	-0.12 ± 0.18	0.69 ± 0.04	3.35 ± 0.11	0.32 ± 0.03	4.53 ± 0.01	0.98 ± 0.02
HD 172140	0.39 ± 0.29	0.53 ± 0.04	2.80 ± 0.15	0.49 ± 0.06	4.58 ± 0.01	0.94 ± 0.02
HD 177989	-0.81 ± 0.21	0.85 ± 0.07	3.10 ± 0.20	0.49 ± 0.07	4.56 ± 0.01	0.99 ± 0.02
HD 178487	-0.32 ± 0.15	0.74 ± 0.04	4.78 ± 0.19	0.32 ± 0.03	4.58 ± 0.01	1.04 ± 0.01
HD 179407	-1.42 ± 0.13	1.03 ± 0.07	3.59 ± 0.19	0.49 ± 0.06	4.60 ± 0.01	1.03 ± 0.02
Average	-0.47	0.66	3.38	0.35	4.58	0.94
Peculiar Velocity Sample (SD region - 2 curves)						
HD 148422	-2.13 ± 0.07	1.36 ± 0.12	3.01 ± 0.23	0.53 ± 0.03	4.58 ± 0.02	0.93 ± 0.00
HD 151990	-1.07 ± 0.09	1.04 ± 0.07	2.19 ± 0.06	0.68 ± 0.06	4.60 ± 0.01	0.81 ± 0.02
HD 158243	-2.20 ± 0.16	1.56 ± 0.22	4.26 ± 0.52	0.55 ± 0.06	4.61 ± 0.02	1.16 ± 0.01
HD 160993	-1.65 ± 0.08	1.43 ± 0.19	3.42 ± 0.31	0.74 ± 0.07	4.72 ± 0.02	1.07 ± 0.01
HD 163522	-3.70 ± 0.20	1.86 ± 0.23	1.18 ± 0.07	0.51 ± 0.10	4.59 ± 0.01	0.74 ± 0.03
HD 164340	-2.96 ± 0.13	1.67 ± 0.28	0.79 ± 0.06	0.76 ± 0.18	4.44 ± 0.02	0.79 ± 0.03
HD 165582	-0.87 ± 0.12	1.10 ± 0.09	2.31 ± 0.14	0.57 ± 0.06	4.61 ± 0.01	0.84 ± 0.01
Average	-1.83	1.19	1.52	0.58	4.60	0.93

(1992). Table 1 lists a value of $E(B-V)$ for each star from Sembach et al. (1993). Table 2 lists the $\Delta(B-V)$ between the measured $(B-V)$ of the reddened star and the $(B-V)_o$ of the best-match dereddened comparison star. The extinction curves for the sample stars are shown in Figure 2.

The extinction curves have been fitted using the Fitzpatrick & Massa (1990, hereafter FM) parameterization. They have developed an analytical representation of the shape of the extinction curves using a small number of parameters. This was done using linear combinations of a Drude bump profile, $D(x; \gamma, x_o)$, a linear background and a far-UV curvature function, $F(x)$, where $x = \lambda^{-1}$. There are 6 parameters determined in the fit: The strength, central wavelength, and width of the bump, c_3 , x_o , and γ , the slope and intercept of the linear background, c_1 and c_2 , and the strength of the far-UV curvature, c_4 . The FM fits to individual extinction curves are plotted in Figure 2 and the best fit parameters for each curve are given in Table 3.

Near-infrared photometry exists for a few of the reddened stars in our sample. For these stars, using JHK photometry, we calculated values of R_V . Due the small values of $E(B-V)$ for our sample stars, the uncertainties in R_V are relatively large. Within these uncertainties, most are consistent with the typical diffuse dust value of 3.1. There is no trend with position on the sky discernible with the small number of sightlines having measured R_V values.

4. DISCUSSION

The sightlines in our sample cover very long distances and have relatively low reddenings so the average densities are amongst the lowest known (Sembach et al. 1993). The measured values for $n_o(\text{H I}) (= N(\text{H I}) \sin |b| / h(\text{H I})$ where $h(\text{H I})$ is the scale height of H I) are listed in Table 1. The parameter, $n_o(\text{H I})$, is a measure of average density along a sightline (Sembach et al. 1993). Typically, when $n_o(\text{H I}) < 0.42 \text{ cm}^{-3}$, no large cold clouds are present along the line of sight (Sembach et al. 1993). All the stars in Table 1 satisfy this criterion. In addition, the warm intercloud medium dominates over the diffuse cold cloud medium if $n_o(\text{H I}) < 0.2 \text{ cm}^{-3}$. Most of the stars in Table 1 satisfy this criterion or come close to it. The ratio of the column density of Ca II to Na I, also listed in Table 1, is another measure of the relative contributions of cloud and intercloud medium. Na I is relatively stronger in clouds while Ca II is relatively strong in the diffuse ISM. This is due to the strong variation in the calcium depletion from the gas phase into dust grains (Sembach & Danks 1994; Crinklaw, Federman, & Joseph 1994). The depletion is higher inside clouds and lower outside where the harsher environment including sputtering and grain collisions will return calcium to the gas phase. The wide range in $N(\text{Ca II})/N(\text{Na I})$ indicates that the cloud/inter-cloud fraction varies strongly from one sightline to another. The absorption features along these lines of sight show multiple components indicating that the distribution of gas is patchy. The average number of components or clouds is 1.5 kpc^{-1} for Na I and 2.0 kpc^{-1} for Ca II (Sembach & Danks 1994). Using these values and the measured reddening, the average $E(B-V)$ per cloud is 0.05 mag which is typical for standard diffuse clouds (Spitzer 1978). Similarly, the average H I column density per cloud is $2.3 \times 10^{20} \text{ cm}^{-2}$. It is

likely that most of these sightlines are dominated by warm intercloud medium and have little contribution from the cold cloud medium.

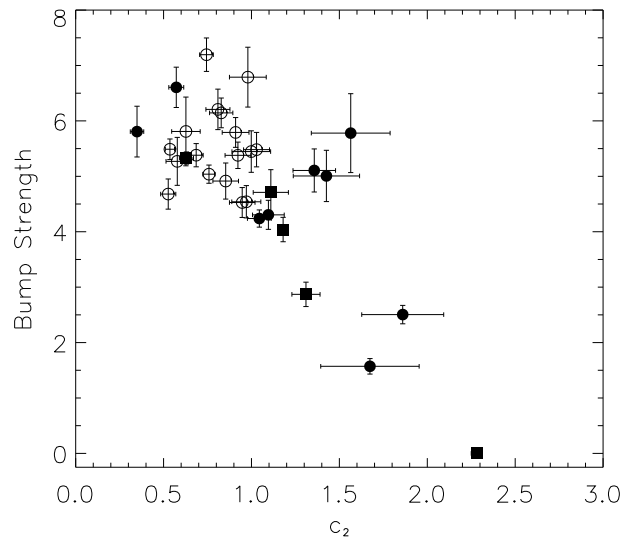


FIG. 3.— The steepness of the far-UV extinction (c_2) plotted against bump strength ($\pi c_3/2\gamma$) for the stars in the SD region lying between $l=325^\circ$ to 0° (filled circles) and those of the rest of the sample (open circles). Also, plotted from upper left to lower right are average points for the Galaxy, the LMC (outside LMC 2), LMC 2 and SMC (Misselt et al. 1999; Gordon & Clayton 1998) (filled squares).

Figure 2 shows that even for extremely diffuse sightlines such as those in our sample, most extinction curves still follow CCM with $R_V = 3.1$. However, there is a subsample of these sightlines whose extinction curves show weak bumps and very steep far-UV extinction similar to the Magellanic clouds. These sightlines all lie in one region of the sky in the direction of the Galactic center. This region (Sembach & Danks 1994 (hereafter the SD region)) coincides with an area of Galactic longitude, $l=325^\circ$ to 0° , where large forbidden velocities have been observed in the gas. Figure 3 shows bump strength plotted against far-UV steepness for our sample extinction curves. The bump strength can be quantified as the area under the bump using the FM parameters to be $\pi c_3/2\gamma$ (Fitzpatrick & Massa 1986). The steepness of the far-UV extinction can be characterized using the FM parameter, c_2 , which represents the slope of the linear background. Seven of the nine sightlines lying in the SD region have the largest values of c_2 in our sample. Six of these sightlines also have bump strengths below the Galactic average. The sightlines in our sample outside the SD region have values of bump strength and c_2 grouped around the Galactic average. As can be seen in Figure 3, the SD region extinction parameters fall roughly along a line running from the average Galactic values through the LMC and LMC 2 averages to the those seen in the SMC. This is a promising result as it indicates that whatever factors are affecting the dust properties in the Magellanic clouds may also be affecting the low density dust in the Milky Way. As discussed below, the two SD-region stars which appear in the upper left-hand corner of Figure 3 do not share the extinction properties of the rest of the SD region sample.

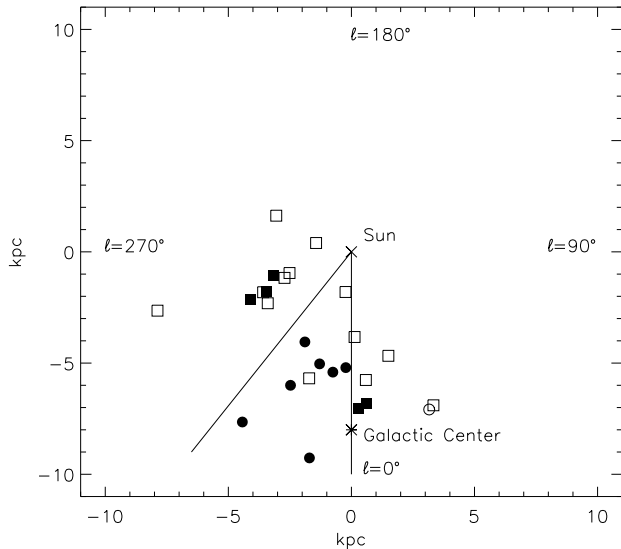


FIG. 4.— The sightlines marked with circles have weak bumps and steep far-UV extinction. The sightlines marked with squares have stronger bumps and less extreme far-UV extinction. Filled circles have $N(\text{Ca II})/N(\text{Na I}) > 0.62$ and $c_2 > 1.0$, open circles have $N(\text{Ca II})/N(\text{Na I}) < 0.63$ and $c_2 > 1.0$, filled squares have $N(\text{Ca II})/N(\text{Na I}) > 0.62$ and $c_2 < 1.0$, open squares have $N(\text{Ca II})/N(\text{Na I}) < 0.63$ and $c_2 < 1.0$. The wedge represents the SD region where forbidden gas velocities were measured by Sembach & Danks (1994).

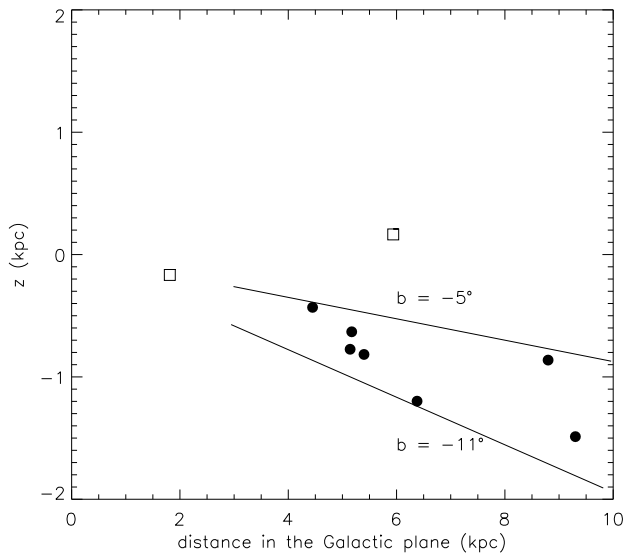


FIG. 5.— Height above or below the Galactic plane plotted against distance in the plane for the stars in the SD region in Figure 4. The symbols are the same as for Figure 4. See text.

The locations of the stars in our sample are plotted in Figure 4. We have separated sightlines according to the steepness of the far-UV extinction as measured by c_2 and also the ratio, $N(\text{Ca II})/N(\text{Na I})$, which measures the relative fraction of cloud and intercloud medium along a sightline. A high value indicates a high fraction of intercloud medium. All of the sightlines in Table 1 with both $N(\text{Ca II})/N(\text{Na I}) > 0.62$ and $c_2 > 1.02$ lie in the SD region. Figure 5 shows height above or below the Galactic plane plotted against distance in the plane for the stars in the SD

region. Figures 4 and 5 clearly show the anomalous extinction is seen only for stars in one particular direction. The two stars in the SD region, that do not share the anomalous extinction of the other sightlines, provide information on the location of this dust. HD 151805 has $b = 1.59^\circ$ so its sightline does not go below the Galactic plane as do the other stars in the sample. HD 161653 lies at a distance of 1.8 kpc and is, by far, the closest star in the $l=325^\circ$ to 0° region. So the dust responsible for the Magellanic-cloud-like extinction lies further than about 2 kpc and in a direction defined by $325^\circ \leq l \leq 0^\circ$ and $-5^\circ \geq b \geq -11^\circ$. In fact, the four sightlines with the steepest extinction, HD 158243, 160993, 163522, and 164340, most resembling the SMC extinction, lie in an even smaller region bounded by $337^\circ \leq l \leq 352^\circ$ and $-8^\circ \geq b \geq -11^\circ$. These four stars also have the lowest reddenings. So the remaining three less-extreme sightlines are likely a combination of clouds including more CCM-like dust as well. Kennedy, Bates, & Kemp (1998) give a nice analysis of the absorption components in this direction of the sky including the sightline to HD 163522 ($l = 349.6$, $b = -9.1$, $d = 9.4$ kpc). In their picture, nearby clouds at 50 pc, 100 pc to 1 kpc, the Sagittarius (1.5-2 kpc) and Scutum-Crux (3 kpc) spiral arms all provide absorption components with negative or small positive velocities. They identify peculiar velocity gas corresponding to the forbidden velocities of $+10$ - 50 km s^{-1} found by Sembach & Danks (1994). These forbidden velocities differ significantly from those expected purely from Galactic rotation. The origin and distance of this gas is not well known. Higher ionization ions are associated with this gas indicating that it may be associated with a Galactic fountain or worm (Savage, Massa, & Sembach 1990; Savage, Sembach, & Cardelli 1994).

The extinction curves for the sightlines inside and outside of the SD region are plotted together in Figure 6. Two sightlines, toward HD 151805 and 161653, in the SD region show normal CCM ($R_V = 3.1$) extinction. As discussed above, the dust along those sightlines is not located in the same volume of space with the SD type dust so they are plotted with the non-SD-region sample in Figure 6. The average SD-region curve (again not including HD 151805 and 161653) is plotted in Figure 7 along with the average Milky Way and Magellanic cloud curves for comparison. The average SD-region curve most resembles the HD 62542 and 210121 curves, seen in Figure 1, as well as the LMC 2 curve. The four steepest SD-region curves resemble the SMC Bar curve in the far-UV but still have stronger bump strengths. These curves show little or no slope change from the near to the far-UV while most other curves seen in Figures 1 and 7 tend to turn up steeply to the blue of the bump.

The environments of the LMC 2 and HD 62542 dust may be quite similar to the SD region dust. All are in diffuse regions subject to shocks and strong UV radiation fields. The sightline to HD 210121 contains one quiescent cloud with $E(B-V) = 0.40$. However, this cloud is located in the halo and shows UV extinction quite similar to the that seen in the SD region. Calcium is heavily depleted indicating that grain destruction has not been an important mechanism in producing the unusual extinction (Welty & Fowler 1992). The low optical depth of the Magellanic sightlines implies that the dust is not well shielded from these environmental pressures. The typical molecular

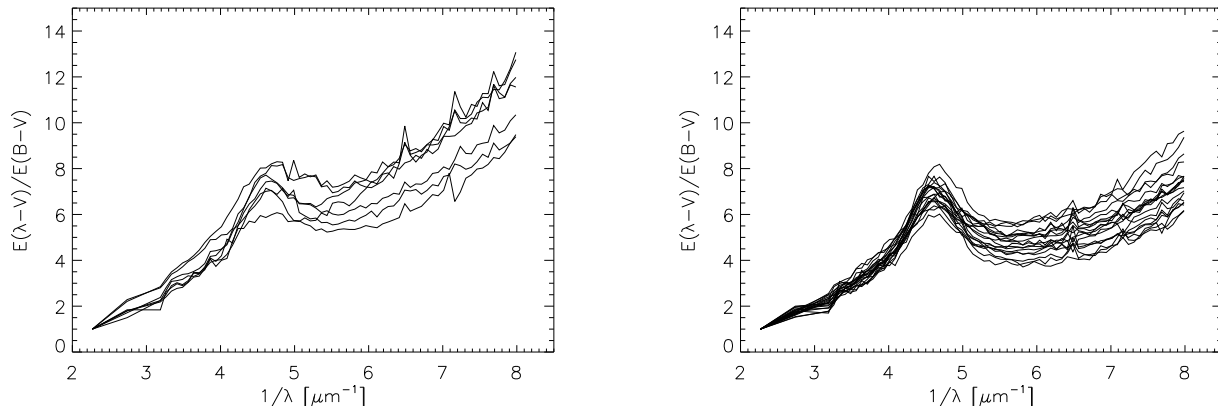


FIG. 6.— The extinction curves for the stars in the SD region (left) and in the rest of the sample (right) are plotted.

cloud in the Magellanic clouds is bigger but more diffuse than in the Galaxy (Pak et al. 1998). Then, the small size of the dust grains in a cloud could be the result of the lack of a very dense environment necessary for the grains to grow through coagulation. This has been suggested as the cause of the anomalous extinction seen along the HD 210121 sightline (Larson et al. 1996; 2000). This kind of low density sightline may mimic the conditions in the SMC where extinction properties have been measured over long sightlines with low values of $E(B-V) = 0.15-0.24$ (Gordon & Clayton 1998). The value of $N(\text{Ca II})/N(\text{Na I})$ is not known for the SMC sightlines but the Ca II abundance in the gas phase is much higher than in the Galaxy for a given reddening (Cohen 1984). The gas-to-dust ratio in general in the SMC is ten times that of the Galaxy (Koornneef 1983). The gas-to-dust ratio in our low density Galactic sample is not significantly different from the average Galactic value (Sembach & Danks 1994). This implies that the gas-to-dust ratio is not well correlated with dust extinction properties.

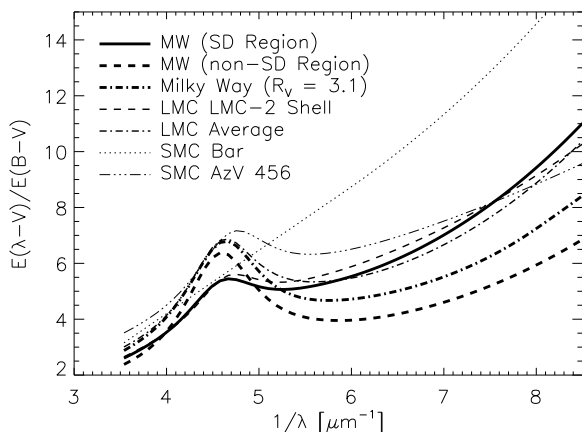


FIG. 7.— Comparison of the average SD region and non-SD region curves with curves for the average MW ($R_V = 3.1$), LMC Average, LMC 2 Shell, SMC Bar, and SMC AzV 456.

The forbidden velocities seen in our sample are associated with warm intercloud material and the turbulent ISM (Sembach & Danks 1994) and may indicate that the dust may have been subject to shocks. Sembach & Savage

(1996) investigated the gas and dust abundances in the halo, finding that they are consistent with progressively more severe processing of grains from the disk into the halo. In addition, they find that while some material is returned to the gas phase, the grain cores seem resistant to destruction. Dust models indicate that the far-UV rise in the extinction curve becomes steeper with increased frequency of exposure to shocks which produces more small dust grains (O'Donnell & Mathis 1997). However, the frequently shocked dust models that produce steeper far-UV extinction also result in stronger bumps. So, producing an SMC-like extinction curve is not as simple as placing dust in a diffuse environment and waiting for a supernova shock.

The next logical step is to attempt to directly connect grain properties to their respective sightline environments. Consequently, we have included the average SD region extinction curve in a comprehensive study of dust in the Local Group where our goal is to explicitly examine the correlation of grain size distributions to sightline characteristics such as depletion patterns, and radiation environment (Wolff et al. 2000).

5. CONCLUSIONS

- Magellanic-cloud-like extinction has now been found in the Milky Way.
- Large values of $N(\text{Ca II})/N(\text{Na I})$ indicating low depletion are associated with steep far-UV extinction as measured by c_2 .
- Global metallicity seems not to be a direct factor. Local environmental conditions seem to be the most important factor in determining dust properties.
- Similar UV dust extinction properties have now been seen in the Milky Way, the Magellanic clouds, starburst galaxies and in high redshift star-forming galaxies.
- There may be at least two ways to achieve similar extinction properties. A lack of dust coagulation has been suggested for HD 210121 to explain the observed extinction (Larson et al. 1996). The Galactic SD-region properties are closely tied to forbidden velocities indicating that processing of the grains in the diffuse ISM resulted in their observed properties.
- There seems to be a correlation between decreasing bump strength and far-UV steepness that includes the Galaxy and the Magellanic Clouds.

• All the sightlines contained in CCM lie within 1 kpc of the Sun. As this study shows, dust properties are not well mapped even in our own Galaxy. There are a larger range of UV extinction parameters seen in the Milky Way than implied by CCM.

Thanks to Ed Fitzpatrick for providing his IUE IDL procedure. This project was originally envisioned by the late Jason Cardelli.

REFERENCES

- Bianchi, L., Clayton, G. C., Bohlin, R. C., Hutchings, J. B., & Massey, P. 1996, *ApJ*, 471, 203
 Cardelli, J.A., & Savage, B.S. 1988, *ApJ*, 235, 864
 Cardelli, J.A., Clayton, G.C., & Mathis, J.S. 1989, *ApJ*, 345, 245
 Cardelli, J.A., & Clayton, G.C. 1991, *AJ*, 101, 1021
 Cardelli, J.A., Sembach, K.R., & Mathis, J.S. 1992, *AJ*, 104, 1916
 Clayton, G.C., & Martin, P.G. 1985, *ApJ*, 288, 558
 Clayton, G.C., and Fitzpatrick, E.L. 1987, *A.J.*, 93, 157
 Clayton, G.C., Green, J., Wolff, M.J., Zellner, N.E.B., Code, A.D., & Davidsen, A.F. 1996, *ApJ*, 460, 313
 Cohen, J.G. 1984, *AJ*, 89, 1779
 Crinklaw, G., Federman, S.R., & Joseph, C.L. 1994, *ApJ*, 424, 748
 Fitzpatrick, E. L. 1985, *ApJ*, 299, 219
 Fitzpatrick, E. L. 1986, *AJ*, 92, 1068
 Fitzpatrick, E. L. & Massa, D. 1986, *ApJ*, 307, 286
 Fitzpatrick, E. L. & Massa, D. 1990, *ApJS*, 72, 163
 Fitzpatrick, E.L. 1999, *PASP*, 111, 63
 Gordon, K. D., Calzetti, D., & Witt, A. N. 1997, *ApJ*, 487, 625
 Gordon, K. D. & Clayton, G. C. 1998, *ApJ*, 500, 816
 Gordon, K.D., Hanson, M.M., Clayton, G.C., Rieke, G.H., & Misselt, K.A. 1999, *ApJ*, 519, 165
 Gordon, K.D., Smith, T.L., & Clayton, G.C. 2000, in "The High-Redshift Universe: Galaxy Formation and Evolution at High Redshift", (ASP Conf. Proceed.), eds. A. J. Bunker & W. J. M. van Breugel, (ASP: San Francisco), in press
 Kennedy, D.C., Bates, B., & Kemp, S.N. 1998, *A&A*, 336, 328
 Kizskurno-Koziej, E., & Lequeux, J. 1987, *A&A*, 185, 291
 Koornneef, J. 1983, *A&A*, 128, 84
 Larson, K.A., Whittet, D.C.B., & Hough, J.H. 1996, *ApJ*, 472, 755
 Larson, K.A., Wolff, M.J., Roberge, W.G., Whittet, D.C.B., & He, L. 2000, *ApJ*, in press
 Massa, D., Savage, B. D., & Fitzpatrick, E. L. 1983, *ApJ*, 266, 662
 Massa, D., & Fitzpatrick, E. L. 2000, *ApJS*, in press
 Mathis, J. S., & Cardelli 1992, *ApJ*, 398, 610
 Mathis, J. S. 1994, *ApJ*, 422, 176
 Misselt, K., Clayton, G.C., & Gordon, K.D. 1999, *ApJ*, 515, 128
 O'Donnell, J.E., & Mathis, J.S. 1997, *ApJ*, 479, 806
 Pak, S., Jaffe, D.T., Van Dishoeck, E.F., Johansson, L.E.B., & Booth, R.S. 1998, *ApJ*, 498, 735
 Pitman, K.M., Clayton, G.C. & Gordon, K.D. 2000, *PASP*, in press
 Savage, B.D., Massa, D., & Sembach, K. 1990, *ApJ*, 355, 114
 Savage, B.D., Sembach, K., & Cardelli, J.A. 1994, *ApJ*, 420, 183
 Sembach, K.R., Danks, A.C., & Savage, B.D. 1993, *A&AS*, 100, 107
 Sembach, K.R., & Danks, A.C. 1994, *A&A*, 289, 539
 Sembach, K.R., & Savage, B.D. 1996, *ApJ*, 457, 211
 Spitzer, L. 1978, *Physical Processes in the Interstellar Medium*, (Wiley & Sons: New York)
 Welty, D.E., & Fowler, J.R. 1992, *ApJ*, 393, 193
 Wolff, M.J., Clayton, G.C., & Gordon, K.D. 2000, in preparation